NEARSHORE WAVE ENERGY

by

M. G. Skafel

Technical Report Number 2

Hydraulics Research Division

Canada Centre for Inland Waters

1973

ABSTRACT

Wave measurements in deep and shallow water off Burlington Bar at the southwest corner of Lake Ontario are described and analyzed. The predicted shallow water wave energy is in semi-quantitative agreement with field measurements. Possible reasons for the discrepancy are discussed.

1. INTRODUCTION

The action of waves in the nearshore region is of major concern to man. Virtually all maritime structures are located in shallow water regions; for example, piers, breakwaters, and offshore drilling platforms. Wave forces are the major cause of shore erosion, littoral drift, and beach formation. Unfortunately, the description of waves in shallow water is not as sophisticated as for those in deep water. When considering nearshore wave problems it is usual to obtain deep water wave information (from wave climate studies or hindcasting techniques) and then to estimate the shallow water conditions by considering the propagation of a 'characteristic' wave into shallow water using linear theory and ignoring wave generation and dissipation in the shallow water. The underlying assumption is that this fictitious characteristic wave (perhaps based on the peak frequency and significant wave height in deep water) somehow provides a suitable model for the propagation of wave energy into shallow water.

In order to obtain field data of wave energy propagation into shallow water and to evaluate prediction methods a wave observation project was initiated in 1972 off Burlington Bar at the southwest corner of Lake Ontario. Wave measurements were made at points located in deep and shallow water. In the latter case the waves were measured

o. ide the breaker zone. Preliminary results show that commonly used prediction procedures can both under and over estimate energy in shallow water.

In Section 2 the field programme is outlined and in Section 3 the prediction procedures described. Field results and nearshore estimates are presented and compared in Section 4. In Section 5 some possible causes for the discrepancies between the predicted and observed shallow water wave energies are discussed.

2. FIELD METHODS

The choice of the field location was governed by two factors. First, it was felt that a site with relatively straight forward bottom contours and a beach on which the wave energy would be dissipated rather than reflected would ease the interpretation of the results. Second, a site close to the Canada Centre for Inland Waters would keep logistic problems simple. The shore off Burlington Bar meets both of these requirements. The bottom contours are relatively straight, and parallel to the shoreline, with a mean slope of about 0.006 (slightly less in deep water, and more very near the shore). In this situation all the wave energy can be assumed to be dissipated on the beach. The site chosen is only a few kilometres from the C.C.I.W. A disadvantage of the site is that the beach faces approximately northeast so is not

suitable for measuring waves due to prevailing westerly winds. However, there are enough storms with north to east winds to make the location practical.

Two transducers were located offshore, one in about 18.3 m of water and one in about 3.7 m of water along a line normal to the shore. The 18.3 m station was about 3 km from shore and 3.7 m station about 0.2 km.

The transducers are accelerometer type buoys (Waveriders) which are only sensitive to vertical accelerations. The acceleration signal was integrated twice in the Waverider and the vertical displacement signal radioed back to a receiver/recorder at the C.C.I.W. The wave records were stored on magnetic tape, which was processed by the personnel of the Wave Climate Study (Department of the Environment and Department of Public Works, Ottawa). The processed data were returned in several formats, the ones of interest here being power density spectra and the significant wave heights, the latter defined as,

$$H_{m_o} = 4(m_o)^{\frac{1}{2}} \qquad (1)$$

where m_o is the zero moment of the power density spectrum.

The procedure adopted during a storm was to record continuously the output of one Waverider for 20 minutes and then switch to the other Waverider. This procedure was repeated for as long as was practical. Thus while both stations were not monitored simultaneously, by monitoring the offshore station first, there was an overlap in observation of the waves due to the wave propagation time between stations.

Each 20 minute record was analyzed by dividing it into eight blocks of 1024 samples and obtaining a power density spectrum for each block. These spectra were averaged to obtain a mean spectrum used for all subsequent calculations.

Hourly averaged wind records were obtained from a point just offshore near the location of the buoys. The wind records were used to estimate the direction of the deep water waves which were taken to be uni-directional and in the direction of the wind.

3. PREDICTION MODELS

Given the deep water spectra, the spectra at the shallow water station were predicted and compared with the observed results. Two methods of predicting the shallow water wave energy were used, both of them assuming linear wave theory, and straight parallel bottom contours. The first method was to calculate the change in each spectral component.

The second method was to assume all the wave energy was contained in a characteristic wave having the frequency of the peak of the spectrum and a wave height equal to the significant wave height.

First order wave theory was used throughout, so the following dispersion relation was applicable for each spectral component;

$$\sigma^2 = gk \tanh kz \tag{2}$$

where σ is the frequency (rad/s), g the gravitational acceleration (m/s^2), k the wave number (m^{-1}), and z the mean depth (m). In deep water, the hyperbolic tangent becomes one and it was taken as one when $kz \geq \pi$.

The usual assumption that the energy flux was everywhere continuous and perpendicular to the crest components was made. Individual rays for each component did not have to be calculated, because the bottom contours were assumed straight and parallel. Instead the ratio of energy density (or power density) for each spectral component between stations at any two depths can be readily found:

$$\frac{E_1}{E_2} = \frac{\tanh k_2 z_2}{\tanh k_1 z_1} \cdot \frac{\sinh 2 k_1 z_1}{\sinh 2k_1 z_1 + 2k_1 z_1} \cdot \frac{\sinh 2k_2 z_2 + 2k_2 z_2}{\sinh 2k_2 z_2} \cdot \frac{\cos \alpha_2}{\cos \alpha_1} \tag{3}$$

(see for example, Wiegel 1964).

The right hand side of equation 3 is simply the ratio of the group velocities at the two depths times the ratio of the cosines of the directions at the two depths relative to the perpendicular to the beach. The latter ratio is obtained from Snell's law, which is:

$$k_1 \sin \alpha_1 = k_2 \sin \alpha_2 \tag{4}$$

Note that the angle α_2 is not determined from the deep water direction, rather the direction at station 2 (in this case the station in 18.3 m of water) after refraction from deep water had been taken into account. It was necessary to use equation 3 instead of the more familiar form, given as:

$$\frac{E_1}{E_2} = \frac{1}{\tanh k_1 z_1} \cdot \frac{\sinh 2k_1 z_1}{\sinh 2k_1 z_1 + 2k_1 z_1} \cdot \frac{\cos \alpha_2}{\cos \alpha_1} \tag{5}$$

because for severe storms a depth of 18.3 m could not be considered deep water. That is, a significant portion of the wave energy had corresponding wavelengths greater than twice 18.3 m.

4. RESULTS

Measurements from two storms were obtained. In figure 1 the hourly averaged wind speed and direction information is summarized and the times of wave measurements indicated. Because the wind was from the east for several hours before wave measurements began for both storms, the deep water wave direction was assumed to be from the east,

corresponding to an angle of 28^{o} to the normal to the beach. The fetch length from the east is the full length of Lake Ontario, approximately 250 km.

The storm of October 31, November 1, 1972 (hereafter referred to as storm 1) was less severe than the one on December 15, 1972 (storm 2), the winds being about one third less in magnitude. The overall form of the spectral densities were similar for both storms. Both sets of spectra were characteristic of fully developed wind waves with a sharp rise to the peak frequency and a slope of approximately -5 (log-log plot) for frequencies greater than the peak. Casual examination of the spectral plots did not indicate any marked difference in the form of the spectra between the deep and shallow water.

Examples for each storm are shown in figures 2 and 3.

The spectra from the two storms differed in two respects. The peak frequency was lower and the total energy greater for storm 2. This result is in accord with any of the forecasting techniques available (see, for example, Technical Report No. 4, 1961). Because the nearshore buoy was at the same depth (3.7 m) for both storms one would expect that the effects of shoaling and refraction to be more important for storm 2 because of the lower frequencies and longer wave lengths. This turns out to be true but other effects appear to influence the results as well.

For storm 1 the peak frequencies were 0.19 Hz for deep and shallow water, while for storm 2 they were in the range 0.13 to 0.14 Hz. The relative intensities of the two storms are exemplified by the range of significant wave heights for the deep water station, 1.0 to 1.3 m for storm 1 and 1.8 to 2.25 m for storm 2. The observed shallow water spectra yielded significant wave heights of similar magnitude as the deep water ones, but there was an interesting difference in the results for the two storms. In storm 1, the significant wave height ranged from 0.8 to 1.1 m, a reduction from deep water. In storm 2, the reverse occurred and the wave heights were increased to the range from 2.2 to 2.4 m.

The significant wave heights for the shallow water station were derived from the deep water spectra in two ways. First the whole shallow water spectra were found using equations 3 and 4 and the corresponding shallow water significant wave height evaluated. Second, the deep water energy was assumed to be concentrated in a characteristic wave based on the peak frequency and significant wave height. The corresponding shallow water wave height was then found directly using equations 3 and 4.

Using the first method the ranges of shallow water wave heights were 0.95 to 1.2 m for storm 1 and 1.85 to 2.35 m for storm 2. Using the second method the results were 0.87 to 0.11 m for storm 1 and 2.1 to 2.95 m for storm 2. The results are shown in Table 1. Both methods indicated the correct trends in wave height, that is, a decrease for storm 1 and an increase for storm 2. The ratios of the zero moments of the spectra are also given in Table 1 to show the relative energies (for the characteristic wave method the predicted shallow water moment was found using equation 1).

The characteristic wave method predicted more closely the shallow water energy for storm 1, overpredicting up to 23% compared to the spectrum method which overpredicted as much as 32%. For storm 2 the characteristic wave method overpredicted as well as underpredicted (+36% to -10%), while the spectrum method always underpredicted (from 2 to 44%).

5. DISCUSSION

The two methods were able to predict correctly whether there would be an increase or a decrease in energy density but neither was particularly accurate in predicting the magnitude. From this result it can be concluded that shoaling and refraction cause significant change in energy density but that other factors are also important and are not included in the model.

One factor that may be significant is bottom friction. This source of dissipation plays an ever increasing role as the ratio of depth to wavelength decreases. While a measure of the bottom friction between the two stations can only be made by the integration of the energy equation for each spectral component an upper bound on it can be estimated by considering the dissipation at constant depth for the characteristic wave.

The dissipation in the laminar boundary layer is given by:

$$D = \left(\frac{2\nu}{\sigma}\right)^{\frac{1}{2}} \cdot \frac{k\sigma E}{\sinh 2kz} \tag{6}$$

where ν is the kinematic viscosity. (Longuet-Higgins, 1970). The dissipation is equal to the loss of energy flux with distance:

$$\frac{\partial}{\partial x} (Ec_g) = -D \tag{7}$$

where c_g is the group velocity. From equations 6 and 7 the ratio of energy between two stations is

$$\frac{E}{E_o} = \exp\left\{2\left(\frac{2\nu}{\sigma}\right)^{\frac{1}{2}} \cdot \frac{k^2 x}{\sinh 2kz + 2kz}\right\} \tag{8}$$

For the characteristic wave of storm 1, depth equal to 3.7 m, and distance equal to 3 km equation 8 indicates an energy loss of about 5%.

Bottom friction models based on a turbulent boundary layer can predict more energy loss, but their usefulness depends critically on the choice of parameters. From the above discussion it appears that bottom friction can account at least in part for the loss in energy density observed in storm 1.

The cause of the increase in energy density in storm 2 is still unresolved. It is possible that first order theory was not suitable for this situation. It has been shown (as noted by Longuet-Higgins, 1956) that for first order theory to be applicable the following inequality must hold:

$$\frac{L^2 a}{z^3} << \frac{16}{3}\pi^2 \qquad (9)$$

where a is the amplitude, L the wavelength, and z the depth, for a monochromatic wave. This relation is not directly useful for a wave spectrum, but it can be used as a crude indication if the amplitude is taken from the significant wave height and the wavelength as that corresponding to the peak frequency. For the observed conditions the left hand side was found to be about 0.1 and 1.0 for storm 1 and 2 respectively, in deep water. In shallow water the corresponding values were about 10 and 40. Criterion 9 is not met for storm 2 in shallow water and consequently predictions based on linear theory may be in error.

Before discarding linear wave theory two other possible causes for the energy density increase should be considered: bottom irregularities which could have resulted in the focusing of energy at the shallow water station; wave generation which would have resulted in a net energy input between stations in storm 2. Both these effects and bottom friction can be included in the energy equation for each spectral component and calculated, as was done by Collins (1972).

In ongoing work more field measurements will be made and studies to improve prediction utilizing the energy equations will be continued.

REFERENCES

Collins, J.I. 1972. Prediction of shallow water spectra. Journal of Geophysical Research 77(15) pp 2693-2707.

Longuet-Higgins, M.S. 1956. The refraction of sea waves in shallow water. Journal of Fluid Mechanics 1 pp 163-176.

Longuet-Higgins, M.S. 1970. An introduction to the study of water waves. Unpublished lecture notes, University of Cambridge.

Technical Report No. 4. 1961. Shore Protection, Planning and Design. U.S. Corps of Engineers, Beach Erosion Board.

Wiegel, R.L. 1964. Oceanographical Engineering. Englewood Cliffs, N.J.: Prentice-Hall

TABLE 1. MEASURED AND PREDICTED WAVE CHARACTERISTICS

Record	Peak Frequency Hz	Significant Wave Height in Metres at Water Depth of:				Ratio of Measured Energy to Predicted Energy	
		18.3 m	3.7 m			$(A/B)^2$	$(A/C)^2$
			Measured (A)	Predicted from 18.3 m spectrum (B)	Predicted from 18.3 m H_{m_o} (C)		
STORM 1							
21.19 EST, 31/10/72	0.19	1.28	1.10	1.19	1.11	0.86	0.98
22.05 " "	0.19	1.22	1.05	1.19	1.06	0.98	0.98
08.39 " 1/11/72	0.19	1.06	0.813	0.986	0.925	0.68	0.77
11.01 " "	0.19	1.01	0.816	0.945	0.870	0.75	0.88
STORM 2							
11.37 EST, 15/11/72	0.14	2.07	2.25	2.12	2.42	1.12	0.87
12.25 " "	0.14	2.15	2.35	2.24	2.52	1.10	0.81
12.46 " "	0.14	1.95	2.18	2.00	2.42	1.19	1.02
13.35 " "	0.14	1.81	2.21	1.84	2.12	1.44	0.68
14.37 " "	0.13 0.15	1.99	2.13	2.02	2.47 2.11	1.10	0.75 1.02
14.58 " "	0.14	1.92	2.37	1.97	2.25	1.44	1.10
16.05 " "	0.13	2.26	2.37	2.35	2.96	1.02	0.64

FIGURE LEGEND

Figure 1. Hourly averaged wind speeds and directions.
Top: storm 1. Bottom: storm 2.

Figure 2. A typical pair of power density spectra for storm 1.
Solid line: 18.3 m of water. Broken line: 3.7 m of water.

Figure 3. A typical pair of power density spectra for storm 2.
Solid line: 18.3 m of water. Broken line: 3.7 m of water.

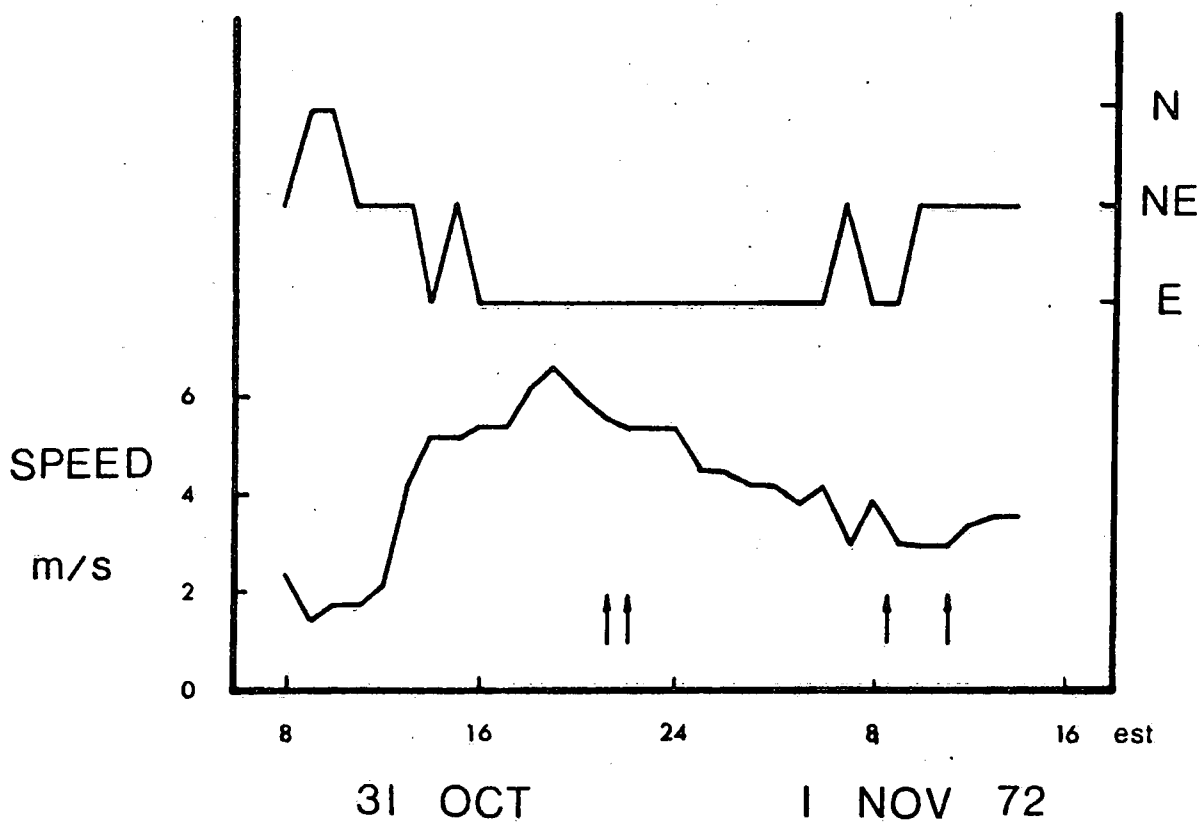
N
NE
E
SPEED
m/s
6
4
2
0
8
16
24
8
16
est
31 OCT
1 NOV 72

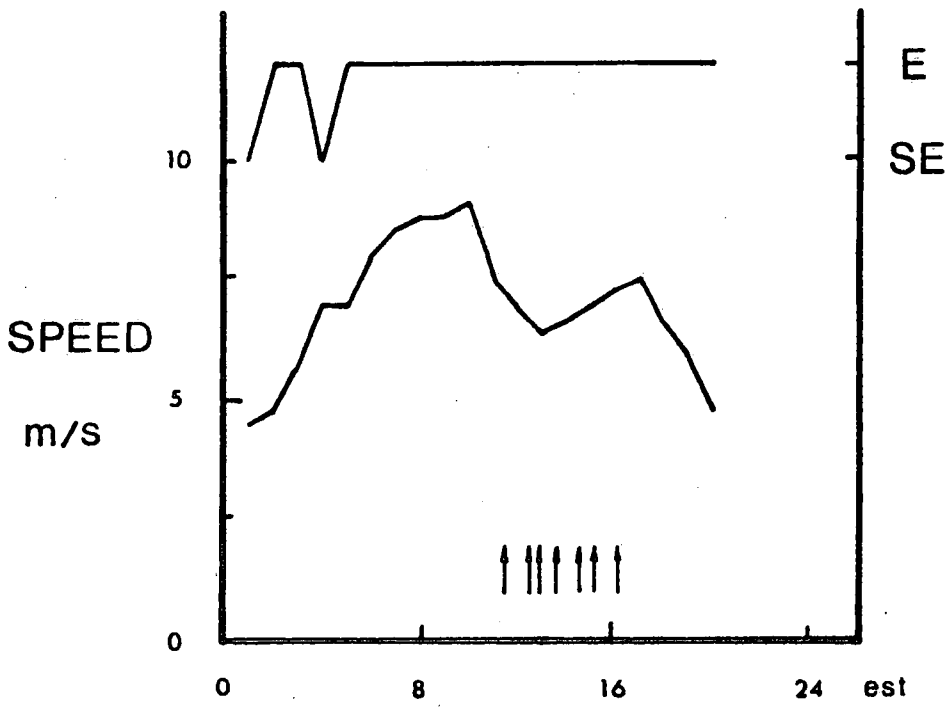
E
SE
SPEED
m/s
10
5
0
0
8
16
24
est
15 DEC 72

Figure 1

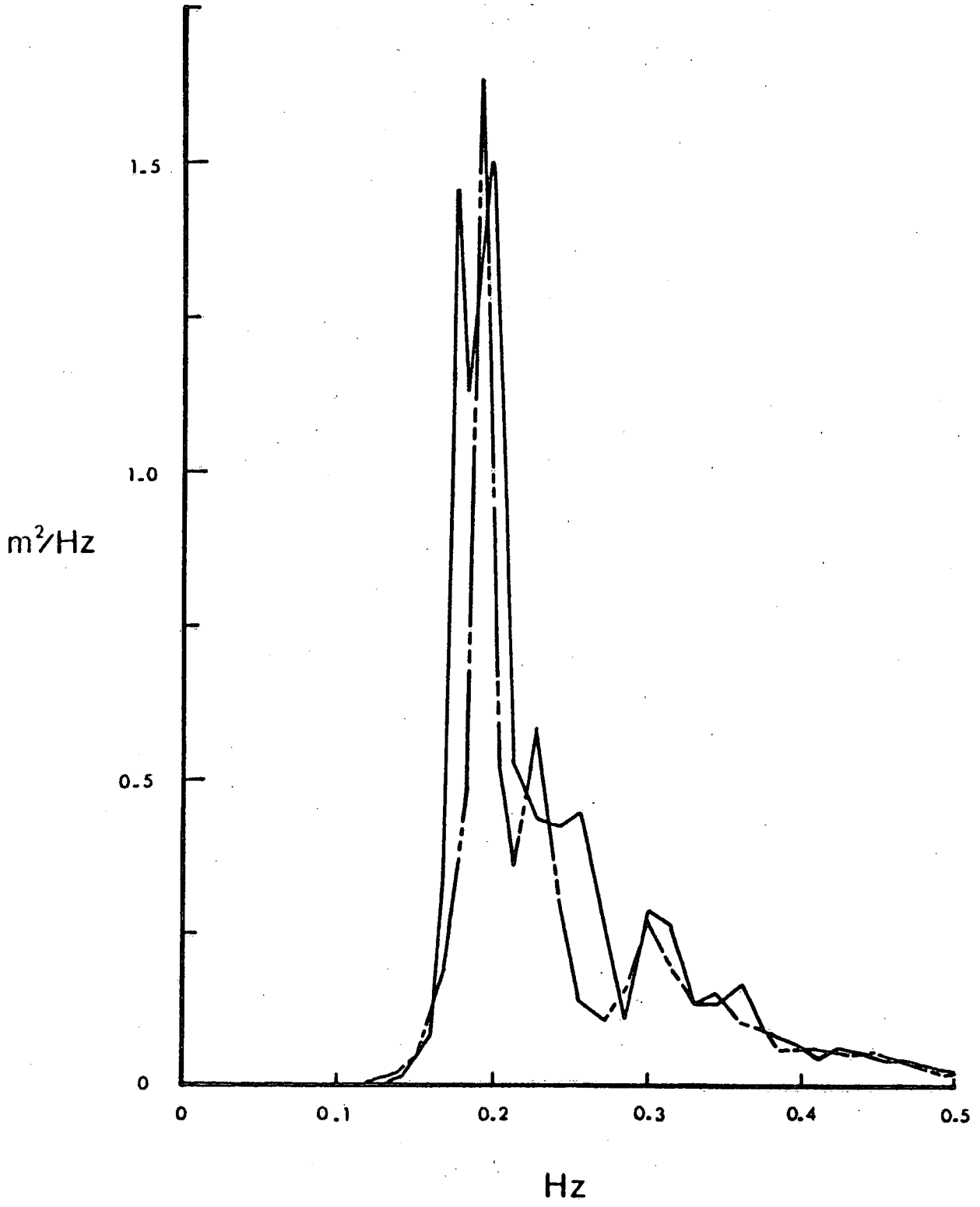

Figure 2

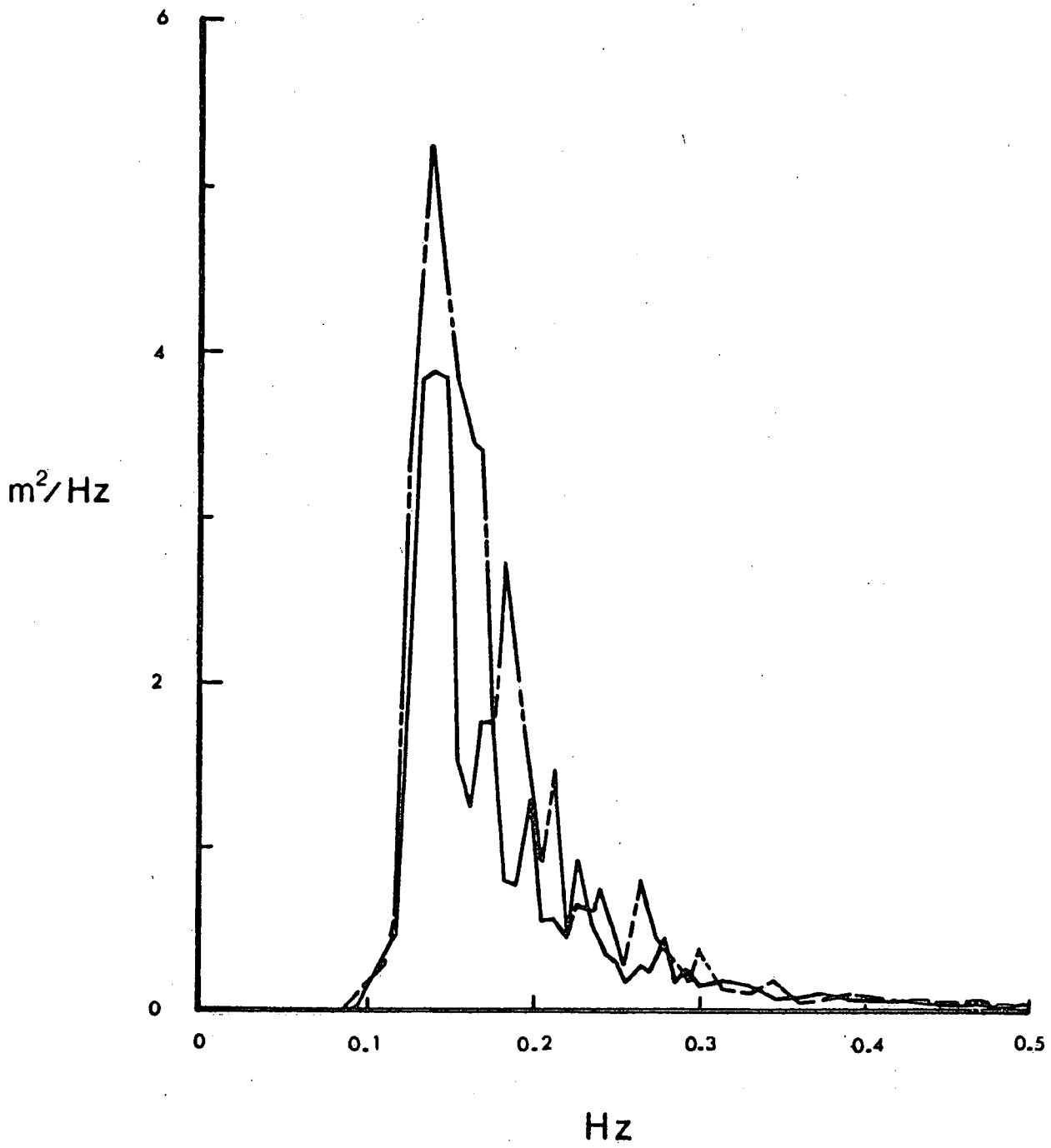

Figure 3